



**HAL**  
open science

## Enchytraeids: Small but important ecosystem engineers

Cécile Serbource, Stéphane Sammartino, Sophie Cornu, Justine Papillon,  
Jérôme Adrien, Céline Pelosi

### ► To cite this version:

Cécile Serbource, Stéphane Sammartino, Sophie Cornu, Justine Papillon, Jérôme Adrien, et al.. Enchytraeids: Small but important ecosystem engineers. *Geoderma*, 2024, 453, pp.117150. 10.1016/j.geoderma.2024.117150 . hal-04867410

**HAL Id: hal-04867410**

**<https://hal.science/hal-04867410v1>**

Submitted on 6 Jan 2025

**HAL** is a multi-disciplinary open access archive for the deposit and dissemination of scientific research documents, whether they are published or not. The documents may come from teaching and research institutions in France or abroad, or from public or private research centers.

L'archive ouverte pluridisciplinaire **HAL**, est destinée au dépôt et à la diffusion de documents scientifiques de niveau recherche, publiés ou non, émanant des établissements d'enseignement et de recherche français ou étrangers, des laboratoires publics ou privés.



Distributed under a Creative Commons Attribution - NonCommercial - NoDerivatives 4.0  
International License



## Enchytraeids: Small but important ecosystem engineers

Cécile Serbource<sup>a,\*</sup>, Stéphane Sammartino<sup>b</sup>, Sophie Cornu<sup>c</sup>, Justine Papillon<sup>d</sup>,  
Jérôme Adrien<sup>d</sup>, Céline Pelosi<sup>a,\*</sup>

<sup>a</sup> Institut National de la Recherche Agronomique (INRAE), Avignon, France

<sup>b</sup> Avignon Université, INRAE, Avignon, France

<sup>c</sup> Aix Marseille Université, CNRS, IRD, INRAE, CEREGE, Aix-en-Provence, France

<sup>d</sup> Institut National des Sciences Appliquées de Lyon, Laboratoire MatÉIS, Lyon, France

### ARTICLE INFO

Handling Editor: Jan Willem Van Groenigen

#### Keywords:

Potworm  
Bioturbation  
Imaging technics  
Connectivity  
Soil engineer

### ABSTRACT

Enchytraeids (Annelida Oligochaeta), small burrowing organisms found worldwide, are known to influence soil structure, though their specific effects on pore space are not well quantified. In this study, we evaluated how the burrowing activities of *Enchytraeus albidus* and *Enchytraeus crypticus* affected the X-ray imaged porosity of soil over a 40-day period using two different soils (loamy and silty-clay-loamy soil) sieved to 2 mm and packed at two bulk densities (0.8 and 1 g cm<sup>-3</sup>). Our findings revealed that while enchytraeids had minimal impact on X-ray imaged porosity, they played a key role in reshaping the soil's internal structure, increasing pore connectivity and homogenizing pore size distribution. This was evident through a reduction in the number of smaller pores and a shift toward larger pore sizes. The overall pore structure became more uniform, with enchytraeids promoting a shift in the dominant pore sizes. These structural changes were particularly pronounced in loosely compacted soils, where enchytraeids contributed to greater network complexity, as well as in the soil with a higher clay content, which is more conducive to aggregation. This suggests that enchytraeids have a significant role in modifying soil physical properties, especially in conditions where the soil is loosely compacted. X-ray microtomography is a promising tool for studying at the mesopore scale, and further studies are needed to better characterize the bioturbation activity of enchytraeids.

### 1. Introduction

Enchytraeids are small (6–50 mm in length) unpigmented Annelida Oligochaeta that belong to the soil mesofauna (body diameter 0.1–2 mm). They can be found in all continents, from the tropics to the polar regions (Didden, 1993), and are bioindicators of chemical stress and agricultural practices because of their sensitivity to environmental changes (Didden and Römbke, 2001; Pelosi and Römbke, 2016). Like earthworms, enchytraeids are recognized as soil engineers due to their effects on soil structure and nutrient availability for other organisms (Bullinger-Weber et al., 2007; Brussaard et al., 2012). Through their burrowing activity, enchytraeids form new pores that affect soil structure (Van Vliet et al., 1998). As Enchytraeids are soft-bodied animals that consume dead organic matter and soil microorganisms (Römbke, 1991; Koutika et al., 2001; Gajda et al., 2017), they are inevitably linked to burrowing activities in the soil. Unlike earthworms (Brown et al., 2000), enchytraeid digging behaviour has not been clearly

characterized. Yet, bioporosity linked to enchytraeid activity has a substantial effect on soil aeration, by significantly enhancing air permeability (Didden et al., 1997; Topoliantz et al., 2000) and elevating the total soil heterotrophic respiration (Lagerlöf et al., 1989). Enchytraeids ingest and transport mineral soil particles, fill soil pores with their excrement, and influence the soil structure and aggregate stability (Didden, 1990; Van Vliet et al., 1993; Tyler et al., 2001). However, research on enchytraeids as bioturbators remains very limited and their effect on soil porosity and structure has never been quantitatively assessed.

X-ray microtomography (XCT) is a non-invasive and non-destructive imaging technique that uses X-rays to create cross-sections of a physical object and enables the reconstruction of 3-D images. Since the 1980 s, this technique has been used to study the morphological properties of the soil structure (Pires et al., 2020; Petrovic et al., 1982). Microtomography is a promising technique to study enchytraeid activity because it can capture images at the mesoscopic scale, which is precisely

\* Corresponding authors.

E-mail addresses: [cecile.serbource@inrae.fr](mailto:cecile.serbource@inrae.fr) (C. Serbource), [celine.pelosi@inrae.fr](mailto:celine.pelosi@inrae.fr) (C. Pelosi).

<https://doi.org/10.1016/j.geoderma.2024.117150>

Received 31 July 2024; Received in revised form 16 December 2024; Accepted 17 December 2024

Available online 30 December 2024

0016-7061/© 2024 Published by Elsevier B.V. This is an open access article under the CC BY-NC-ND license (<http://creativecommons.org/licenses/by-nc-nd/4.0/>).

the scale range at which enchytraeids operate (Mermillod-Blondin et al., 2018). Yet, only one study used XCT to analyse the enchytraeid pore network (Porre et al., 2016), where soil columns of 6.7 cm in diameter and 14 cm in depth to assess the synergy between soil organisms (i.e., *Enchytraeus albidus*, fungivorous and predatory mites) for greenhouse gas emissions. The study design did not give priority to the enchytraeid pore network, no structural indicator were calculate and so characterization and did not allow concluding on their influence on soil physical properties.

The aim of this study was to characterize the burrowing activity of enchytraeids using two different species [*E. albidus* (20–30 mm long, diameter 0.6–1 mm in width at the clitellum) and *Enchytraeus crypticus* (3–12 mm long, diameter 0.18–0.30 mm in width at the clitellum)] (Westheide and Graefe, 1992; Schmelz and Collado, 2010; Nagy et al., 2023) and to quantify their impact on soil imaged porosity and structure in repacked soil columns in laboratory conditions. Two soils (loamy and silty-clay-loamy) were tested at two bulk densities (0.8 and 1 g cm<sup>-3</sup>). XCT provided 3-D images at the start and 40 days after enchytraeid introduction (or control, i.e. no animal). These images were analyzed for imaged porosity, connectivity (Euler number), exchange surfaces, and pore size distribution to determine if enchytraeids modify pore space based on soil texture and bulk density.

## 2. Material and methods

### 2.1. Preparation of the soil columns

To simulate an arable system, two calcareous soils (Table 1) were used: a loamy soil and a silty-clay-loamy soil (IUSS Working Group WRB, 2022). The soils were manually affined, air-dried and passed through a 2 mm sieve.

Water Holding Capacity (WHC) is defined by the ability of a certain soil texture to physically hold water against the force of gravity. Both soils were moistened to 60 % of their respective WHC with tap water and then sieved again through a 2 mm sieve. Smaller grain sizes (i.e. soil sieved at 500 µm, 800 µm, 1 mm) and higher bulk densities (i.e. 1.1, 1.2, 1.4 g cm<sup>-3</sup>) were tested in the early stages of this study showing that enchytraeids cannot enter these soils. Sixteen cylindrical plastic vessels (3.3 cm in diameter and 6.0 cm in height) were filled with the soils to reach a total height of 2.5 cm. For each soil, eight columns were used, four packed at a bulk density of 0.8 g cm<sup>-3</sup> and four at 1 g cm<sup>-3</sup>. The soil moisture was adjusted to 80 % WHC by carefully and homogeneously dropping water at the top of the column.

The chosen bulk densities correspond to the topmost soil horizon rich in organic matter, the typical habitat of enchytraeids (Davidson et al., 2002; Rasoulzadeh and Yaghoubi, 2010; Murphy, 2015).

### 2.2. Enchytraeids

*E. albidus* individuals were bought from AQUAPLANTE (sold as fish food) and *E. crypticus* individuals came from a breeding culture at INRAE

**Table 1**  
Characteristics of the two soils used in the experiment.

	Loamy soil	Silty-clay-loamy soil
Site name	Valabre Agricultural College	Avignon INRAE centre
Site coordinates	43.464304, 5.451139	43.943437, 4.865881
Land use	Vineyard	Grassy pear orchard
pH (H <sub>2</sub> O)	8.1	8.3
Clay (%)	24	29
Silt (%)	36	52
Sand (%)	40	18
Soil Organic Carbon (g kg <sup>-1</sup> )	22.4	15.4
Total nitrogen (g kg <sup>-1</sup> )	2.35	1.77
Water holding capacity (%)	38.2	26.0

Avignon, France. Both species were successfully maintained in our laboratory in the dark at 18 °C for several months (in soil and on agar-agar, respectively) and fed finely ground rolled oats twice per week.

For each soil bulk density, one vessel remained without enchytraeids (control). For each treatment with enchytraeids (two soils, two bulk densities), three replicates were used in which 10 *E. albidus* (equivalent to 12 000 individuals m<sup>-2</sup>) and 120 *E. crypticus* (equivalent to 140 000 individuals m<sup>-2</sup>) adults were introduced. These abundances are realistic according to what has been reported in arable fields (1000 to 100 000 individuals m<sup>-2</sup> in cropland) (Beylich and Achazi 1999; Beylich and Graefe, 2012; Ricci et al. 2015) and respect the distribution of small and large organisms at 80 % and 20 % (Edwards and Bohlen, 1996), respectively, while ensuring that juveniles comprised 60 % of the total annelid population (Curry and Schmidt, 2007). Parafilm was attached by an elastic band at the top of each column to ensure gas exchange and maintain the soil moisture, while preventing enchytraeid escape during the experiment. The sixteen columns were kept in a dark room at constant temperature (18 °C) for 40 days. Weekly, 10 mg of powdered oatmeal was placed on the soil surface as food source for the enchytraeids. The soil moisture was adjusted weekly at 80 % WHC by weighing the columns and adding water when necessary.

### 2.3. Image acquisition

The columns were scanned by XCT at the experiment start (here named T0, before the introduction of enchytraeids) and at day 40 (named Tf). A GE Phoenix v|tome|x s tomograph (INSA Lyon, France) was used. The tube voltage was set to 120 kV and the intensity to 120 µA “FAST” category acquisition using a continuous rotation were performed, with a voxel size of 20 µm for a total of 1500 projections. An optical copper filter of 0.3 mm of thickness was added. The exposure time employed was 0.666 s, giving a total acquisition time of 17 min per 3-D scan. The X-ray source was perpendicular to the columns. The cone-beam XCT data were reconstructed by a filtered back projection Feldkamp-algorithm using the PHOENIX datosx 2 software to compute the slices.

### 2.4. Image analysis

The raw 3-D images were processed using Fiji. First, a region of interest (ROI) of 19x19x14 mm<sup>3</sup> (950x950x701 voxels) centred to the raw volume to avoid edge effects was selected in each column (Fig. 1A). The ROIs in the columns with enchytraeids at bulk density of 0.8 g cm<sup>-3</sup> (both soils) were adjusted individually to avoid pixels of air due to the column surface collapse at Tf (Table 2, Fig. 1B).

The greyscale distribution was then normalized and equalized, and a median filter of 1 voxel size was applied to reduce the noise. Each 3-D image was multiplied by itself to further increase the contrast between organic matter and pores. Imaged porosity thresholding was performed automatically to avoid operator-related effects. The global threshold was determined according to the so-called “Minimum” algorithm based on the histogram shape (Prewitt and Mendelsohn, 1966). The resulting image is a binary (8-bit greyscale) 3-D image with pores at a grey level of 0 and the solid phase (to which organic matter is associated) at 255. Thresholding quality was estimated by the operator based on two aspects: (i) the good superposition of the pore edges on the grey level image, and (ii) organic matter association with the solid phase (Fig. S1). These controls, carried out on two central vertical planes of the 3-D image, indicated that the thresholding approach yielded reasonable results.

As proposed by Vogel et al. (2010), a binary structure can be characterized by several basic geometric measures, named Minkowski functionals. Some of them have been used to characterize the activity of enchytraeids and to associate basic geometric properties with the column meso-structure: total imaged pore volume or X-ray imaged porosity percentage when divided by the sample volume ( $\epsilon$ ); vertical distribution

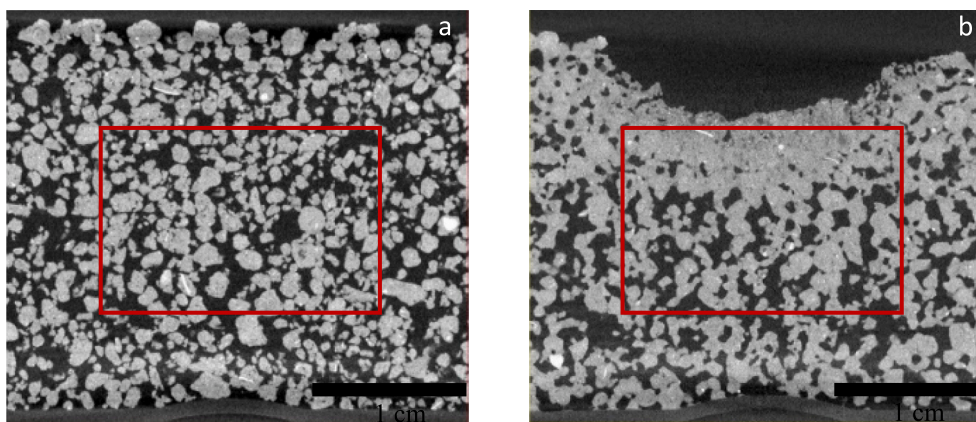


**Fig. 1.** Two X-ray microtomography images of soil cross-sections showing the region of interest delineation (red rectangle) in a column of silty-clay-loamy soil (bulk density 0.8 g cm<sup>-3</sup>) at the beginning of the experiment (T0) (A) and at the end of the experiment (Tf; 40 days with enchytraeids)(B). (For interpretation of the references to colour in this figure legend, the reader is referred to the web version of this article.)

**Table 2**

Number of slides considered for image analysis of the two soils (L, loamy soil; SCL, silty-clay-loamy soil) and bulk densities at the beginning (T0) and end (Tf) of the experiment.

Soil	Column replicate	0.8		1	
		Number of slices analysed T0	Number of slices analysed Tf	Number of slices analysed T0	Number of slices analysed Tf
L	Control	701	701	701	701
	R1	701	668	701	701
	R2	701	691	701	701
	R3	701	648	701	701
SCL	Control	701	701	701	701
	R1	701	672	701	701
	R2	701	637	701	701
	R3	701	602	701	701

of the imaged porosity profile; total interfacial area between pore and solid or specific surface when divided by the total sample volume ( $S_V$ ); and Euler number calculated using the number of isolated objects (closed convex) minus the number of redundant connections or loops (closed saddle surfaces) plus the number of cavities (closed concave). The Euler number is a connectivity indicator: a positive number in-

the data (with a degree of freedom equal to 10) and negative values were adjusted to zero to eliminate any non-physical value. The skewness coefficient was calculated from the smoothed data to assess the distribution asymmetry. A high skewness coefficient indicates the predominance of smaller or larger pores, suggesting a less uniform pore size distribution, whereas a low skewness coefficient implies a more homogeneous distribution. For each modality, the mode was identified and the corresponding class refers to the dominant pore size category. This information is functionally significant because it helps to determine the prevalent pore size that contributes most to the soil structure, by influencing properties such as aeration, water infiltration, and root penetration.

When the conditions for parametric tests were met (normality of residues using the Shapiro-Wilk test and homogeneity of variance using the F test), the Student's *t*-test was used. When these conditions were not met, logarithmic or square root transformations were used, and if the conditions for the parametric tests were still not met, the initial (T0) and final (Tf) values of the different indicators were compared with the Wilcoxon test (R Development Core Team 2018).

The imaged porosity variation of each slide (Table 2) was calculated, considering the difference between the imaged porosity at T0 and Tf, with the following formula:

$$\text{Imaged porosity variation (\%)} = \left( \frac{\text{Final state porosity} - \text{Initial state porosity}}{\text{Initial state porosity}} \right) * 100$$

indicates a predominance of isolated components compared with redundant connections. A negative Euler number indicates the predominance of redundant connections. Lastly, the pore size distribution was characterized using the local thickness algorithm. The local pore diameters within the pore space were deduced with the maximum inscribed sphere method (Hildebrand and Rügsegger, 1997). All these features were measured at T0 (initial state) and Tf (40 days after adding or not the enchytraeids).

### 2.5. Data treatment

For the columns with enchytraeids, the mean  $\pm$  standard deviation (SD) of the three replicates was used.

Pore size distribution according to the column depth was smoothed using a moving average and grouped into 50  $\mu$ m size classes to eliminate part of the variability. Then, a spline interpolation was used to smooth

The imaged porosity variation of each slide was graphically represented (Fig. 2) to determine whether enchytraeids differently affected imaged porosity according to the column depth. In the control columns, imaged porosity variation was homogeneous at the different depths (Fig. 2A). This variability in control columns was considered as noise because it was not linked to enchytraeid activity, but to sample moving during the experiment, particularly transport by car. Only imaged porosity variations larger than the variation range ( $-2.66 \pm 6.25$ ; mean  $\pm$  SD) in the control columns were considered as resulting from enchytraeid activity. To be as conservative as possible and not over-interpret the results, 2 SD were kept to define the noise (Fig. 2B).

### 3. Results

In the four control columns without enchytraeids, total imaged

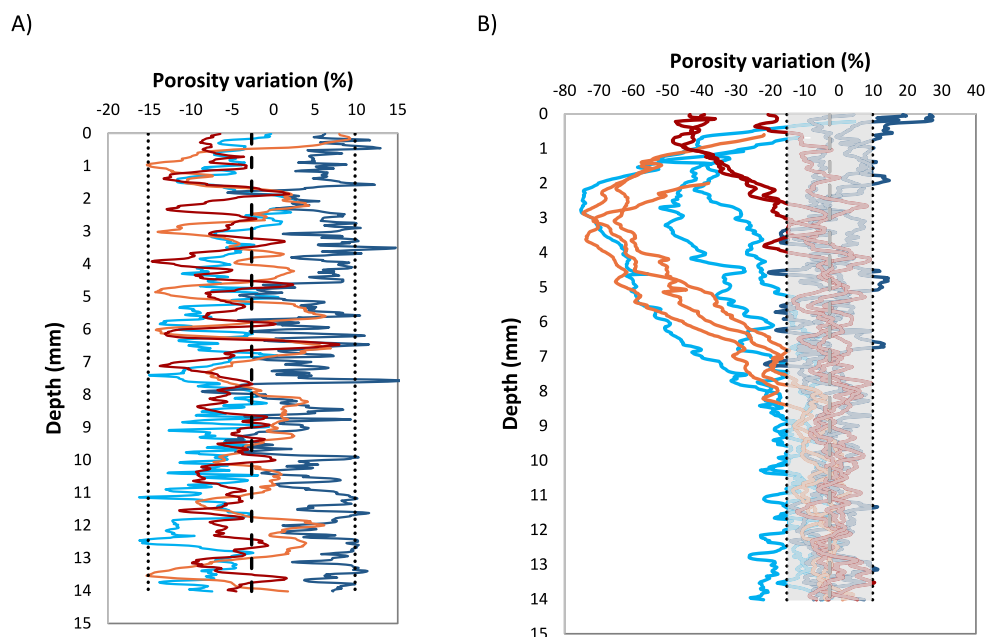


**Fig. 2.** Porosity variation (%) in function of the column depth (mm) between the beginning (T0) and end (Tf) of the experiment in: (A) the control columns (without enchytraeids) and (B) the columns with enchytraeids. Light blue, loamy soil at the bulk density of  $0.8 \text{ g cm}^{-3}$ ; dark blue, loamy soil at the bulk density of  $1 \text{ g cm}^{-3}$ ; orange, silty-clay-loamy soil at the bulk density of  $0.8 \text{ g cm}^{-3}$ ; red, silty-clay-loamy soil at the bulk density of  $1 \text{ g cm}^{-3}$ . The mean porosity variations in the control columns  $\pm 2 \text{ SD}$  are represented with dashed and dotted lines, respectively, in (A) and as a grey area in (B). (For interpretation of the references to colour in this figure legend, the reader is referred to the web version of this article.)

**Table 3**

Total soil porosity (in percentage, mean  $\pm \text{SD}$  in columns with enchytraeids) and Euler number at the beginning (T0) and end (Tf) of the experiment for the loamy soil and silty-clay-loamy soil at two bulk densities in the control columns (without animals) and in the columns with enchytraeids; n, number of replicates; \* indicates a significant difference between T0 and Tf values.

Soil	Bulk density ( $\text{g.cm}^{-3}$ )	Treatment	n	Total porosity (%)		Euler number	
				T0	Tf	T0	Tf
Loamy	0.8	Control	1	36.8	34.5	- 65,256	- 62,467
		Enchytraeids	3	$36.8 \pm 0.7$	$28.1 \pm 3.2$	- 62,535	- 4332 *
	1	Control	1	28.6	29.9	- 60,914	- 63,562
		Enchytraeids	3	$27.8 \pm 1.7$	$27.3 \pm 2.5$	- 55,464	- 21,999 *
Silty-clay-loamy	0.8	Control	1	43.6	42.2	- 11,986	- 11,886
		Enchytraeids	3	$43.6 \pm 0.4$	$32.7 \pm 2.1$	* - 11,204	- 1546 *
	1	Control	1	36.9	35.0	- 14,636	- 11,757
		Enchytraeids	3	$36.0 \pm 2.1$	$35.5 \pm 2.7$	- 13,190	- 9385.7

porosity was lower in the loamy soil than in the silty-clay-loamy soil, whatever the bulk density (Table 3). The pore volume did not change between T0 and Tf in the four control columns (Table 3) and in the columns with enchytraeids, except in the silty-clay-loamy soil at the bulk density of  $0.8 \text{ g cm}^{-3}$  where it decreased by 11 % (Student's *t*-test,  $p\text{-value} = 2.6 \times 10^{-6}$ ).

The Euler number was negative in all columns, indicating a highly interconnected pore space. The values were higher in the silty-clay-loamy soil than in the loamy soil (Table 3). Moreover, from T0 to Tf, the Euler number increased by 93 % (Student's *t*-test,  $p\text{-value} = 3.8 \times 10^{-5}$ ) and 86 % (Student's *t*-test,  $p\text{-value} = 6.6 \times 10^{-4}$ ) in the loamy and silty-clay-loamy soils with enchytraeids (bulk density of  $0.8 \text{ g cm}^{-3}$ ), respectively (Table 3). At the highest bulk density, the difference between T0 and Tf was significant only in the loamy soil, with an increase by 60 % (Student's *t*-test,  $p\text{-value} = 3.2 \times 10^{-2}$ ) (Table 3).

The imaged porosity variation tended to decrease in the zone of enchytraeids activity, more in the silty-clay-loamy soil than in the loamy soil and more for the bulk density of  $0.8$  than for  $1 \text{ g cm}^{-3}$  (Fig. 2B). At the bulk density of  $0.8 \text{ g cm}^{-3}$ , both soils displayed a significant decrease in imaged porosity over the first 8 mm: the mean maximum imaged porosity loss ranged from 40 % (loamy soil) to 7 % (silty-clay-

loamy soil) (Fig. 2B). At 8 mm of depth, the imaged porosity variation was of the same order of magnitude than in the control columns. At the bulk density of  $1 \text{ g cm}^{-3}$ , the imaged porosity variation in the silty-clay-loamy soil decreased over the first 3 mm, and the maximum imaged porosity loss of 45 % was observed at  $\sim 1 \text{ mm}$  of depth (Fig. 2B). At  $\geq 3 \text{ mm}$  of depth, the imaged porosity variation was of the same order of magnitude than in the control columns. The soil imaged porosity variation in the loamy soil at the bulk density of  $1 \text{ g cm}^{-3}$  was of the same order of magnitude than in the control columns (Fig. 2B).

The pore size distributions were unimodal and each featured a single mode (one peak). In the control columns, the pore size distribution was similar at T0 and Tf as well as the skewness coefficient (Fig. 3A-D). In the loamy soil, the pore size distribution was narrower than in the silty-clay-loamy soil and the pore size was smaller, whatever the bulk density. Increasing the bulk density slightly shifted the distribution towards smaller pore sizes (Fig. 3). Enchytraeid activity showed significant interactions with their environment and altered the soil structure, resulting in a modification of the pore size distribution curve between T0 and Tf. Regardless of the soil type and bulk density, the mode (pore size distribution peak) was less narrow and pronounced and also shifted towards larger sizes, indicating that enchytraeids homogenized the pore

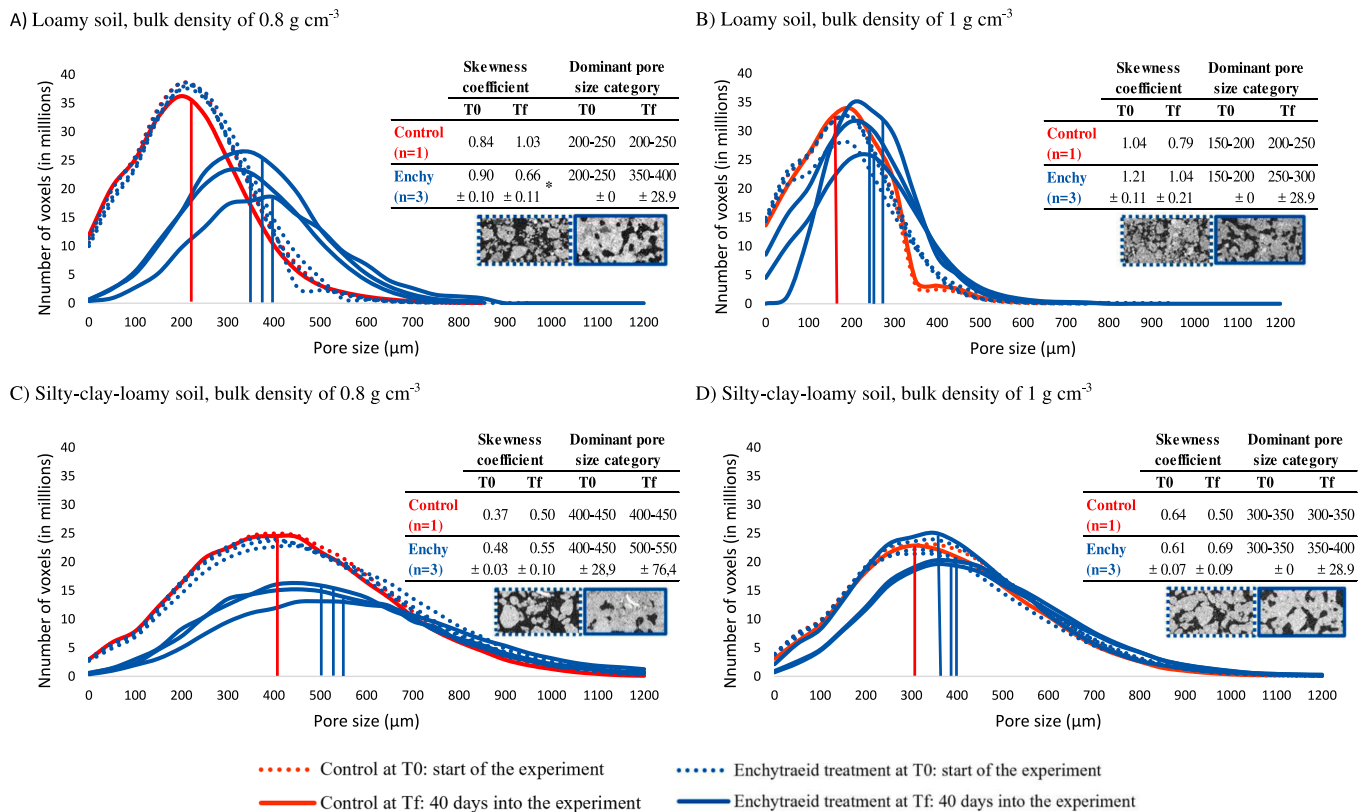


**Fig. 3.** Pore size distributions (50  $\mu\text{m}$  classes) in the control columns (without enchytraeids; in red) and in the columns with enchytraeids (in blue) at the beginning (T0 – dotted lines) and at the end of the experiment (Tf – solid lines), and results of the comparison of the skewness coefficient, dominant pore size category and number of voxels in the dominant pore size category between T0 and Tf in the loamy soil samples at bulk density of 0.8 g cm<sup>-3</sup> (A) and 1 g cm<sup>-3</sup> (B) and the silty-clay-loamy soil samples at bulk density of 0.8 g cm<sup>-3</sup> (C) and 1 g cm<sup>-3</sup> (D); vertical lines represent the peak at T0 (red) and at Tf (blue) in the columns with enchytraeids; n is the number of replicates; \* indicates a significant difference ( $p = 0.05$ ). The images in each panel are microtomography photographs (cross-sections; cropped) of the relevant soil at T0 (left, dotted line) and Tf (right, solid line). (For interpretation of the references to colour in this figure legend, the reader is referred to the web version of this article.)

distribution in the soil. The creation of larger pores, while conserving the overall pore volume, reduced the total number of smaller pores. This shift explains the curve flattening at Tf compared with T0. This is represented by a notable reduction of the mode intensity comparing before and after the work of enchytraeids at the bulk density of 0.8 g cm<sup>-3</sup> for the loamy soil and silty-clay-loamy soil ( $-42.8\%$ , student's  $t$ -test,  $p$ -value =  $2.2 \times 10^{-2}$ , and  $-37.3\%$ , student's  $t$ -test,  $p$ -value =  $4.5 \times 10^{-3}$ , respectively) and a shift of the dominant pore size range from 200–250  $\mu\text{m}$  to 350–400  $\mu\text{m}$  (Fig. 3A) and from 350–400  $\mu\text{m}$  to 450–500  $\mu\text{m}$  (Fig. 3C), respectively. These effects were almost absent in both soils at the bulk density of 1 g cm<sup>-3</sup> (Fig. 3B, D).

All skewness coefficients were positive and ranged between 0.37 and 1.29, indicating highly asymmetric pore size distributions in which smaller pores dominated and extended towards larger ones (Fig. 3A–D). Enchytraeid burrowing activity decreased the skewness coefficient in the loamy soil at the bulk density of 0.8 g cm<sup>-3</sup>, from  $0.90 \pm 0.10$  to  $0.66 \pm 0.11$  (Student's  $t$ -test,  $p$ -value =  $4.8 \times 10^{-2}$ ) (Fig. 3A).

#### 4. Discussion

Imaging techniques, such as tomography (Le Bayon et al., 2021) and microtomography (Balseiro-Romero et al. 2020), have been widely used to study the burrowing activity of earthworms and rarely to explore enchytraeid activity in soils (Porre et al. 2016). Here, we showed that microtomography provides a detailed view of the combined arrangement of pores and solids, allowing us to quantify some changes induced by the activity of enchytraeids, and providing a valuable visual perspective on the interactions between enchytraeids and their

environment. This approach opens new possibilities for better understanding enchytraeid roles and effects in terrestrial ecosystems. The comparison of images acquired at different time points (start and end of the experiment) revealed that the change in total imaged porosity of the control columns without enchytraeids was negligible and that its slight decrease may be explained by the column transport by car between Avignon and Lyon (approx. 200 km) due to vibrations and slightly rearrangement of the aggregates. However, it should be noted that all samples were transported together and were meticulously packed with a focus on shock-absorption procedures.

The densities chosen for this study were based on preliminary results that are not presented in this study. Smaller aggregate sizes (500  $\mu\text{m}$ , 630  $\mu\text{m}$ , 800  $\mu\text{m}$  and 1000  $\mu\text{m}$ ) and higher bulk densities (i.e. 1.1, 1.2, 1.4 g cm<sup>-3</sup>) revealed that even when enchytraeids were combined, the bigger individuals of *E. albidus* (600–1000  $\mu\text{m}$  in width) were unable to penetrate the soil. At a bulk density of 1 g cm<sup>-3</sup>, enchytraeids burrowed through the entire soil volume, as indicated by the noticeable bioporosity on images (Fig. S2). Enchytraeids could be considered as “porosity opportunists” because they use the voids already present in the soil. Therefore, unlike earthworms, the studied species of enchytraeids cannot be considered as true diggers. Retractor muscles in enchytraeids are not as developed as in earthworms (Weir Bell, 1962). We used species adapted to loose environments that naturally live in loose material. Using species representative of mineral soils might yield different results.

In the present study, we found that *E. albidus* and *E. crypticus*, working in synergy through their burrowing activity, did not change the total imaged porosity, with the exception of the silty-clay-loamy soil at low bulk density (0.8 g cm<sup>-3</sup>) (decrease by 10%). Therefore, the soil type and bulk

density influenced the enchytraeid effect on soil imaged porosity. Specifically, enchytraeids had more pronounced physical effects in the silty-clay-loamy soil (29 % of clay and 18 % of sand) that is more conducive to aggregation than the loamy soil (24 % of clay and 40 % of sand). These organisms burrow and ingest mineral and organic soil particles (van Vliet et al., 1995), secrete mucus and expulse excrements (Karaban and Uvarov, 2014). Excrements can obstruct pores (Didden, 1990) and mucus may act as a binder between soil aggregates, causing particle clumping and creating a more compact structure. This compact structure was observed particularly at the bulk density of  $0.8 \text{ g cm}^{-3}$ , through the entire column depth (Fig. S2). This imaged porosity decrease may also be linked to overpopulation because many juveniles were observed near the surface and at the column edges at the end of the experiment. The high density of adults introduced in the soil columns and the potential high activity of new hatchlings may have influenced (i.e. decreased) imaged porosity. Similarly, van Vliet et al. (1998) observed an increase in larger pores (diameter  $> 147 \text{ }\mu\text{m}$ ) when few enchytraeids were present. However, this effect disappeared after 2 months, due to the large number of enchytraeids and finally, pores were smaller. In future studies, it would be interesting to decrease the number of introduced enchytraeids to see whether the observed effects remain the same.

The Euler number indicated a complex and highly interconnected pore space made by enchytraeids, as observed by Didden (1990) who found that *Enchytraeus buchholzi* increases the continuity and volume of pores corresponding to its body size (50—200  $\mu\text{m}$  pore diameter). Our images showed that the soil of the columns with enchytraeids was highly interconnected. Euler numbers were higher in silty-clay-loamy soil than in loamy soil, indicating that pores in loamy soil were more interconnected. The presence of enchytraeids contributed to increase these values, suggesting that they reduce the number of interconnection paths and therefore act to simplify the complexity of the pore space. This effect was stronger at the lower soil bulk density ( $0.8 \text{ g cm}^{-3}$ ). This could be again explained by their potential greater ease of movement in this looser soil.

The imaged porosity profiles showed that the surface crusts experienced a loss of up to 70 % in total imaged porosity (at the bulk density of  $0.8 \text{ g cm}^{-3}$ ), particularly in the first 8 mm. This may be attributed to the surface feeding activity of enchytraeids during the experiment. Food that was added weekly to the surface (as recommended in the guidelines OECD, 2004) could have been the cause of overactivity in the first 3 mm and overpopulation (many juveniles). Moreover, related to this, large mucus and excrement deposits may have resulted in a much higher local water content and compaction than in the rest of the column. This behaviour may not necessarily reflect the enchytraeid natural habits. Future research should consider not feeding the enchytraeids during the experiment to avoid behavioural changes.

In both loamy and silty-clay-loamy soils, the pore size distributions in the control columns were similar at T0 and T<sub>f</sub>, indicating a relative stability of the porous structure in the absence of enchytraeids. Once again, the minimal modification observed at the bulk density of  $1 \text{ g cm}^{-3}$  in both soils (Fig. 3B, D) could be attributed to reduced passage of enchytraeids in denser soils. Their intensive work generates a slight increase in fine macro-porosity, shifting the size distribution of the remaining pores towards larger sizes (Fig. 3), although the total pore volume decreased due to compaction or aggregation. In the presence of enchytraeids, the pore size distributions were more symmetrical in loamy soil (both bulk densities) than the before state and therefore, the pore space became more homogeneous. Moreover, enchytraeids increased the overall pore size. The significant changes in pore size distribution and mode highlighted the enchytraeid role in modifying the soil structure. The observed decrease in the mode intensity in the presence of enchytraeids indicates that their bioturbation and burrowing activities resulted in the compaction of some areas and the creation of voids in others, reorganizing the soil structure by reducing the number of larger pores and creating smaller pores. The obtained “spongy” soil structure made by enchytraeids has already been reported by some “old” studies (Jegen, 1920; Kubienna, 1955; Didden, 1991).

The use of two enchytraeid species (*E. albidus* and *E. crypticus*), one small and one larger, represent the size diversity observed in enchytraeid communities in natural soils (Didden, 1991; Schmelz and Collado, 2010). Small enchytraeids may be more agile and have easier access to soil microhabitats, while large enchytraeids may influence more the soil structuring due to their ability to move larger amounts of material. In this experiment, we used relatively high densities of enchytraeids, although based on existing abundances. Considering the limited depth of the experimental columns (2.5 cm), this density probably exacerbated the effects that would be observed under natural field conditions. This setup was chosen to maximize observable effects, given the highly novel nature of this research topic, aiming to provide initial insights and establish a foundation for future investigations under more realistic conditions, such as deeper and more heterogeneous soil environments. The two enchytraeid species used in this experiment are typically regarded as standard test organisms in various guidelines, such as those of the Organization for Economic Development (OECD, 1984) and International Organization for Standardization (ISO, 1993; 1998; 2019). The use of wild species would have been more ecologically relevant, but natural enchytraeid populations are difficult to breed.

## 5. Conclusion

This study revealed the impact of the combined activity of *E. albidus* and *E. crypticus* on soil imaged porosity and structure using advanced imaging techniques (X-ray microtomography). By assessing the enchytraeid behaviour in small disturbed soil columns filled with two different soil types at two different bulk densities, this study unveiled changes at the mesoscopic scale and brings new insights into their environmental interactions with soil properties, such as porosity, compaction, and soil structure modification. The densities chosen for this study were informed by previous findings that indicated enchytraeids may struggle to penetrate soils under certain conditions—specifically with higher bulk densities and smaller aggregate sizes—limiting their ability to create burrows due to increased soil resistance. In our experiment conditions (i.e. aggregates 2 mm), enchytraeids had only a minimal impact on the X-ray imaged porosity, but they significantly affected the soil’s internal structure by increasing pore connectivity and homogenizing pore size distribution. Enchytraeid activity promoted the formation of larger pores that increased the fine macro-porosity. Additionally, the “spongy” soil structures observed in this study are in line with historical findings, indicating a consistent impact of enchytraeid activity on soil properties. This study underscores the functions performed by soil engineers that contribute to the functioning and health of agricultural soils. Incorporating these insights into predictive models can enhance our understanding of the soil structure dynamics and improve land management strategies.

## CRediT authorship contribution statement

**Cécile Serbource:** Writing – review & editing, Writing – original draft, Visualization, Methodology, Investigation, Formal analysis, Data curation, Conceptualization. **Stéphane Sammartino:** Writing – review & editing, Writing – original draft, Visualization, Validation, Supervision, Software, Methodology, Formal analysis, Data curation, Conceptualization. **Sophie Cornu:** Writing – review & editing, Supervision, Investigation, Formal analysis. **Justine Papillon:** Writing – review & editing, Software, Methodology. **Jérôme Adrien:** Writing – review & editing, Software, Methodology. **Céline Pelos:** Writing – review & editing, Writing – original draft, Visualization, Validation, Supervision, Resources, Project administration, Methodology, Investigation, Funding acquisition, Conceptualization.

## Declaration of competing interest

The authors declare that they have no known competing financial

interests or personal relationships that could have appeared to influence the work reported in this paper.

## Acknowledgments

The authors thank the PACA region and INRAE AgroEcoSystem Department for PhD funding.

## Appendix A. Supplementary data

Supplementary data to this article can be found online at <https://doi.org/10.1016/j.geoderma.2024.117150>.

## Data availability

Data will be made available on request.

## References

- Balseiro-Romero, M., Mazurier, A., Monoshyn, D., Baveye, P.C., Clause, J., 2020. Using X-ray microtomography to characterize the burrowing behaviour of earthworms in heterogeneously polluted soils. *Pedobiologia* 83, 150671. <https://doi.org/10.1016/j.pedobi.2020.150671>.
- Beylich, A., Achazi, R.K., 1999. Influence of low soil moisture on enchytraeids. *Newsletter on Enchytraeidae* 6, 49–58.
- Beylich, A., Graefe, U., 2012. Relationships between microannelid and earthworm activity. In: Schrader, S., Schmelz, R.M. (Eds.), *Newsletter on Enchytraeidae*, 12, *Landbauforschung, vTI Agriculture and Forestry Research, Special Issue 357*. Thünen-Institut, Braunschweig, pp. 1–12.
- Brown, G.G., Barois, I., Lavelle, P., 2000. Regulation of soil organic matter dynamics and microbial activity in the drilosphere and the role of interactions with other edaphic functional domains. *European Journal of Soil Biology* 36, 177–198. [https://doi.org/10.1016/S1164-5563\(00\)01062-1](https://doi.org/10.1016/S1164-5563(00)01062-1).
- Brussaard, L., Aanen, D.K., Briones, M.J.I., Decaëns, T., de Deyn, G.B., Fayle, T.M., James, S.W., Nobre, T., 2012. Biogeography and phylogenetic community structure of soil invertebrate ecosystem engineers: global to local patterns, implications for ecosystem functioning and services and global environmental change impacts. *Soil Ecology Ecosystems Services* 201–232. <https://doi.org/10.13140/2.1.3088.2240>.
- Bullinger-Weber, G., Le Bayon, R.-C., Guenat, C., Gobat, J.-M., 2007. Influence of some physicochemical and biological parameters on soil structure formation in alluvial soils. *European Journal of Soil Biology* 43, 57–70. <https://doi.org/10.1016/j.ejsobi.2006.05.003>.
- Curry, J.P., Schmidt, O., 2007. The feeding ecology of earthworms – A review. *Pedobiologia* 50 (6), 463–477.
- Davidson, D.A., Bruneau, P.M.C., Grieve, I.C., Young, I.M., 2002. Impacts of fauna on an upland grassland soil as determined by micromorphological analysis. *Applied Soil Ecology* 20, 133–143. [https://doi.org/10.1016/S0929-1393\(02\)00017-3](https://doi.org/10.1016/S0929-1393(02)00017-3).
- Didden, W.A.M., 1990. Involvement of Enchytraeidae (Oligochaeta) in soil structure evolution in agricultural fields. *Biology and Fertility of Soils* 9, 152–158. <https://doi.org/10.1007/BF00335799>.
- Didden, W.A.M., 1991. Population ecology and functioning of Enchytraeidae in some arable farming systems. Agricultural University Wageningen, The Netherlands, p. 117. Ph.D. Dissertation.
- Didden, W.A.M., 1993. Ecology of terrestrial Enchytraeidae. *Pedobiologia* 37, 2–29.
- Didden, W.A.M., Fründ, H.-C., Graefe, U., 1997. Enchytraeids. Fauna in Soil Ecosystems: Recycling Processes, Nutrient Fluxes, and Agricultural Production. Marcel Dekker Inc, New York, pp. 135–172.
- Didden, W., Römbke, J., 2001. Enchytraeids as indicator organisms for chemical stress in terrestrial ecosystems. *Ecotoxicology and Environmental Safety* 50, 25–43. <https://doi.org/10.1006/eesa.2001.2075>.
- Edwards, C.A., Bohlen, P.J., 1996. *Biological activity in soils*. Wiley, New York.
- Gajda, L., Gorgoň, S., Urbisz, A.Z., 2017. Food preferences of enchytraeids. *Pedobiologia* 63, 19–36. <https://doi.org/10.1016/j.pedobi.2017.06.002>.
- Hildebrand, T., Rügsegger, P., 1997. A new method for the model-independent assessment of thickness in three-dimensional images. *Journal of Microscopy* 185, 67–75. <https://doi.org/10.1046/j.1365-2818.1997.1340694.x>.
- ISO (International Organisation for Standardization). 1993. Effects of pollutants on earthworms (Eisenia fetida). Part 1: Determination of acute toxicity using artificial soil substrate – No. 11268-1. Geneva.
- ISO (International Organisation for Standardization). 1998. Effects of pollutants on earthworms (Eisenia fetida). Part 2: Determination of effects on reproduction – No. 11268-2. Geneva.
- ISO (International Organisation for Standardization). 2019. Soil quality - Guidance on the choice and evaluation of bioassays for ecotoxicological characterization of soils and soil materials – No. 17616. Geneva.
- IUSS Working Group WRB, 2022. World Reference Base for Soil Resources. International soil classification system for naming soils and creating legends for soil maps, 4th edition. International Union of Soil Sciences (IUSS), Vienna, Austria.
- Jegen, G., 1920. Die Bedeutung der Enchytraeiden für die Humusbildung. *Landw. Jahrb. Schweiz* 34, 55–71.
- Karaban, K., Uvarov, A.V., 2014. Non-trophic effects of earthworms on enchytraeids: An experimental investigation. *Soil Biology and Biochemistry* 73, 84–92. <https://doi.org/10.1016/j.soilbio.2014.02.006>.
- Koutika, L.-S., Didden, W.A.M., Marinissen, J.C.Y., 2001. Soil organic matter distribution as influenced by enchytraeid and earthworm activity. *Biology and Fertility of Soils* 33, 294–300. <https://doi.org/10.1007/s003740000323>.
- Kubienna, W.L., 1955. Animal activity in soils as a decisive factor in establishment of humus forms. In: *Soil Zoology*. Butterworth, London, pp. 73–82.
- Lagerlöf, J., Andren, O., Paustian, K., 1989. Dynamics and contribution to carbon flows of enchytraeidae (oligochaeta) under four cropping systems. *The Journal of Applied Ecology* 26, 183. <https://doi.org/10.2307/2403660>.
- Le Bayon, R., Guenat, C., Schlaepfer, R., Fischer, F., Luiset, A., Schomburg, A., Turberg, P., 2021. Use of X-ray microcomputed tomography for characterizing earthworm-derived belowground soil aggregates. *European Journal of Soil Science* 72, 1113–1127. <https://doi.org/10.1111/ejss.12950>.
- Mermillod-Blondin, F., Bouvarot, M., Déjollat, Y., Adrien, J., Maire, E., Lemoine, D., Marmonier, P., Volatier, L., 2018. Influence of tubificid worms on sediment structure, benthic biofilm and fauna in wetlands: A field enclosure experiment. *Freshwater Biology* 63, 1420–1432. <https://doi.org/10.1111/fwb.13169>.
- Murphy, B.W., 2015. Impact of soil organic matter on soil properties—a review with emphasis on Australian soils. *Soil Research* 53, 605. <https://doi.org/10.1071/SR14246>.
- Nagy, H., Dózsa-Farkas, K., Felföldi, T., 2023. New insights into the *Enchytraeus albidus* complex (Annelida, Enchytraeidae), with the description of three new species from seashores in Italy and Croatia. *EJT* 870. <https://doi.org/10.5852/ejt.2023.870.2123>.
- OECD. 1984. Guidelines for the Testing of Chemicals No. 207. Earthworm, Acute toxicity tests. Organisation for Economic Co-operation and Development, Paris.
- OECD. 2004. Guidelines for the Testing of Chemicals No. 220. Enchytraeid reproduction test. Organisation for Economic Co-operation and Development, Paris.
- Pelosi, C., Römbke, J., 2016. Are enchytraeids (Oligochaeta, Annelida) good indicators of agricultural management practices? *Soil Biology and Biochemistry* 100, 255–263. <https://doi.org/10.1016/j.soilbio.2016.06.030>.
- Petrovic, A.M., Siebert, J.E., Rieke, P.E., 1982. Soil bulk density analysis in three dimensions by computed tomographic scanning. *Soil Science Society of America Journal* 46, 445–450. <https://doi.org/10.2136/sssaj1982.03615995004600030001x>.
- Pires, L.F., Auler, A.C., Roque, W.L., Mooney, S.J., 2020. X-ray microtomography analysis of soil pore structure dynamics under wetting and drying cycles. *Geoderma* 362, 114103. <https://doi.org/10.1016/j.geoderma.2019.114103>.
- Porre, R.J., Van Groenigen, J.W., De Deyn, G.B., De Goede, R.G.M., Lubbers, I.M., 2016. Exploring the relationship between soil mesofauna, soil structure and N<sub>2</sub>O emissions. *Soil Biology and Biochemistry* 96, 55–64. <https://doi.org/10.1016/j.soilbio.2016.01.018>.
- Prewitt, J.M.S., Mendelsohn, M.L., 1966. The analysis of cell images. *Annals of the New York Academy of Sciences* 128, 1035–1053. <https://doi.org/10.1111/j.1749-6632.1965.tb11715.x>.
- R Development Core Team (2018): R: A Language and Environment for Statistical Computing. – Vienna, Austria: the R Foundation for Statistical Computing. ISBN: 3-900051-07-0. Available online at <http://www.R-project.org/>.
- Rasoulzadeh, A., Yaghoubi, A., 2010. Effect of cattle manure on soil physical properties on a sandy clay loam soil in North-West Iran. *Journal of Food, Agriculture & Environment* 8, 976–979.
- Ricci, F., Bentze, L., Montagne, D., Houot, S., Pelosi, C., 2015. Positive effects of alternative cropping systems on terrestrial Oligochaeta (Clitellata, Annelida). *Soil Organisms* 87, 71–83.
- Römbke, J., 1991. Estimates of the Enchytraeidae (Oligochaeta, Annelida) contribution to energy flow in the soil system of an acid beech wood forest. *Biology and Fertility of Soils* 11, 255–260. <https://doi.org/10.1007/BF00335844>.
- Schmelz, R.M., Collado, R., 2010. A guide to European terrestrial and freshwater species of Enchytraeidae (Oligochaeta). *Soil Organisms* 82, 1–176.
- Topoliantz, S., Ponge, J.-F., Viaux, P., 2000. Earthworm and enchytraeid activity under different arable farming systems, as exemplified by biogenic structures. *Plant and Soil* 225, 39–51. <https://doi.org/10.1023/A:1026537632468>.
- Tyler, A.N., Carter, S., Davidson, D.A., Long, D.J., Tipping, R., 2001. The extent and significance of bioturbation on 137Cs distributions in upland soils. *Catena* 43, 81–99. [https://doi.org/10.1016/S0341-8162\(00\)00127-2](https://doi.org/10.1016/S0341-8162(00)00127-2).
- Van Vliet, P.C.J., West, L.T., Hendrix, P.F., Coleman, D.C., 1993. The influence of Enchytraeidae (Oligochaeta) on the soil porosity of small microcosms. *Geoderma*, Elsevier Science Publishers B.V. Amsterdam 56, 287–299.
- Van Vliet, P.C.J., Beare, M.H., Coleman, D.C., 1995. Population dynamics and functional roles of Enchytraeidae (Oligochaeta) in hardwood forest and agricultural ecosystems. *Plant Soil* 170, 199–207. <https://doi.org/10.1007/BF02183067>.
- Van Vliet, P.C.J., Radcliffe, D.E., Hendrix, P.F., Coleman, D.C., 1998. Hydraulic conductivity and pore-size distribution in small microcosms with and without enchytraeids (Oligochaeta). *Applied Soil Ecology* 9, 277–282. [https://doi.org/10.1016/S0929-1393\(97\)00053-X](https://doi.org/10.1016/S0929-1393(97)00053-X).
- Vogel, H.-J., Weller, U., Schlüter, S., 2010. Quantification of soil structure based on Minkowski functions. *Computers & Geosciences* 36, 1236–1245. <https://doi.org/10.1016/j.cageo.2010.03.007>.
- Weir Bell, A., 1962. Enchytraeids (Oligochaeta) from Various Parts of the World. *Transactions of the American Microscopical Society* 81, 158. <https://doi.org/10.2307/3223675>.
- Westheide, W., Graefe, U., 1992. Two new terrestrial Enchytraeus species (Oligochaeta, Annelida). *Journal of Natural History* 26, 479–488. <https://doi.org/10.1080/00222939200770311>.